

**This is a self-archived version of an original article. This version may differ from the original in pagination and typographic details.**

**Author(s):** Porcar-Castell, Albert; Malenovský, Zbyněk; Magney, Troy; Van Wittenberghe, Shari; Fernández-Marín, Beatriz; Maignan, Fabienne; Zhang, Yongguang; Maseyk, Kadmiel; Atherton, Jon; Albert, Loren P.; Robson, Thomas Matthew; Zhao, Feng; Garcia-Plazaola, Jose-Ignacio; Ensminger, Ingo; Rajewicz, Paulina A.; Grebe, Steffen; Tikkanen, Mikko; Kellner, James R.; Ihalainen, Janne A.; Rascher, Uwe;

**Title:** Chlorophyll a fluorescence illuminates a path connecting plant molecular biology to Earth-system science

**Year:** 2021

**Version:** Accepted version (Final draft)

**Copyright:** © 2021, Springer Nature Limited

**Rights:** In Copyright

**Rights url:** <http://rightsstatements.org/page/InC/1.0/?language=en>

**Please cite the original version:**

Porcar-Castell, A., Malenovský, Z., Magney, T., Van Wittenberghe, S., Fernández-Marín, B., Maignan, F., Zhang, Y., Maseyk, K., Atherton, J., Albert, L. P., Robson, T. M., Zhao, F., Garcia-Plazaola, J.-I., Ensminger, I., Rajewicz, P. A., Grebe, S., Tikkanen, M., Kellner, J. R., Ihalainen, J. A., . . . Logan, B. (2021). Chlorophyll a fluorescence illuminates a path connecting plant molecular biology to Earth-system science. *Nature Plants*, 7(8), 998-1009. <https://doi.org/10.1038/s41477-021-00980-4>

1 **Chlorophyll-a fluorescence illuminates a path connecting plant molecular biology to Earth-**  
2 **system science**

3

4 Albert Porcar-Castell<sup>1\*</sup>, Zbyněk Malenovský<sup>2</sup>, Troy Magney<sup>3</sup>, Shari Van Wittenberghe<sup>1,4</sup>, Beatriz  
5 Fernández-Marín<sup>5</sup>, Fabienne Maignan<sup>6</sup>, Yongguang Zhang<sup>7</sup>, Kadmiel Maseyk<sup>8</sup>, Jon Atherton<sup>1</sup>,  
6 Loren P. Albert<sup>9, 10</sup>, Thomas Matthew Robson<sup>11</sup>, Feng Zhao<sup>12</sup>, Jose-Ignacio Garcia-Plazaola<sup>13</sup>, Ingo  
7 Ensminger<sup>14</sup>, Paulina A. Rajewicz<sup>1</sup>, Steffen Grebe<sup>15</sup>, Mikko Tikkanen<sup>15</sup>, James R. Kellner<sup>9, 16</sup>, Janne  
8 A. Ihalainen<sup>17</sup>, Uwe Rascher<sup>18</sup>, Barry Logan<sup>19</sup>

9

10 <sup>1</sup>Optics of Photosynthesis Laboratory, Institute for Atmospheric and Earth System Research/Forest  
11 Sciences, Viikki Plant Science Center, University of Helsinki, Helsinki, Finland.

12 <sup>2</sup>School of Geography, Planning, and Spatial Sciences, College of Sciences Engineering and  
13 Technology, University of Tasmania, Private Bag 76, Hobart, TAS 7001, Australia.

14 <sup>3</sup>Department of Plant Sciences, University of California, Davis. Davis, CA, 95616 United States of  
15 America.

16 <sup>4</sup>Laboratory of Earth Observation, University of Valencia, C/Catedrático José Beltrán, 2, 46980  
17 Paterna, Spain.

18 <sup>5</sup>Department of Botany, Ecology and Plant Physiology, University of La Laguna (ULL), Tenerife  
19 38200, Spain.

20 <sup>6</sup>Laboratoire des Sciences du Climat et de l'Environnement, LSCE/IPSL, CEA-CNRS-UVSQ,  
21 Université Paris-Saclay, Gif-sur-Yvette, France.

22 <sup>7</sup>International Institute for Earth System Sciences, Nanjing University, Nanjing, Jiangsu 210023,  
23 China.

24 <sup>8</sup>School of Environment, Earth and Ecosystem Sciences, The Open University, Milton Keynes MK7  
25 6AA, United Kingdom.

26 <sup>9</sup>Institute at Brown for Environment and Society, Brown University, Providence, RI 02912, United  
27 States of America.

28 <sup>10</sup>Biology Department, West Virginia University, Morgantown, WV 26506-6300, United States of  
29 America.

30 <sup>11</sup>Organismal and Evolutionary Biology, Viikki Plant Science Centre (ViPS), Faculty of Biological  
31 and Environmental Science, 00014, University of Helsinki, Finland.

32 <sup>12</sup>School of Instrumentation Science and Opto-Electronics Engineering, Beihang University,  
33 Beijing, 100083, China.

34 <sup>13</sup>Department of Plant Biology and Ecology, University of the Basque Country (UPV/EHU),  
35 Bilbao, Spain.

36 <sup>14</sup>Department of Biology, Graduate Programs in Cell & Systems Biology and Ecology &  
37 Evolutionary Biology, University of Toronto, 3359 Mississauga Road, Mississauga, ON L5L 1C6,  
38 Canada.

39 <sup>15</sup>Molecular Plant Biology, University of Turku, FI-20520 Turku, Finland.

40 <sup>16</sup>Department of Ecology and Evolutionary Biology, Brown University, Providence RI 02912,  
41 United States of America.

42 <sup>17</sup>Nanoscience Center, Department of Biological and Environmental Science, University of  
43 Jyväskylä, Jyväskylä 40014, Finland.

44 <sup>18</sup>Institute of Bio- and Geosciences, Plant Sciences (IBG-2), Forschungszentrum Jülich GmbH,  
45 Jülich, Germany.

46 <sup>19</sup>Biology Department, Bowdoin College, Brunswick, Maine, United States of America.

47

48 \*Corresponding author: [joan.porcar@helsinki.fi](mailto:joan.porcar@helsinki.fi)

49

50

51 **For decades, the dynamic nature of chlorophyll-a fluorescence (ChlaF) has provided insight**  
52 **into the biophysics and ecophysiology of the light reactions of photosynthesis from the**  
53 **subcellular to leaf scales. Recent advances in remote sensing methods now enable detection of**  
54 **ChlaF induced by sunlight across a range of larger scales, using instruments mounted on**  
55 **towers above plant canopies to Earth-orbiting satellites. This signal is referred to as *solar-***  
56 ***induced fluorescence* (SIF) and its application promises to overcome spatial constraints on**  
57 **studies of photosynthesis, opening new research directions and opportunities in ecology,**  
58 **ecophysiology, biogeochemistry, agriculture and forestry. However, to unleash the full**  
59 **potential of SIF, intensive cross-disciplinary work is required to harmonize these new**  
60 **advances with the rich history of biophysical and ecophysiological studies of ChlaF, fostering**  
61 **the development of next-generation plant physiological and Earth system models. Here, we**  
62 **introduce the scale-dependent link between SIF and photosynthesis, with an emphasis on**  
63 **seven remaining scientific challenges, and present a roadmap to facilitate future collaborative**  
64 **research towards new SIF applications.**

65 When illuminated, chlorophyll-a molecules weakly emit light in the 650-850 nm range; that is, they  
66 fluoresce. Steady state<sup>1,2</sup> and time-resolved fluorescence spectroscopy<sup>3,4</sup>, as well as pulse-amplitude  
67 modulated (PAM) fluorescence<sup>5,6</sup> have long been used by biophysicists, molecular biologists and  
68 ecophysiologicalists to elucidate the structure and function of the photosynthetic apparatus<sup>7-9</sup>. These  
69 techniques are regarded as active because the measured ChlaF originates from a controlled light  
70 source, and accordingly have largely<sup>10,11</sup> been restricted to measurements at the subcellular and leaf  
71 levels.

72 Interest in passive remote sensing methods capable of retrieving solar-induced ChlaF across a  
73 continuum of spatial scales emerged more than two decades ago<sup>12</sup>. These seminal activities led to  
74 the first demonstrations of tower-based<sup>13,14</sup> and satellite<sup>15</sup> SIF measurements over terrestrial  
75 ecosystems. The opportunity to remotely detect an energy flux (Box 1) that arises directly from



76 within the photosynthetic process spurred the rapid development of measurement techniques,  
77 retrieval protocols, and models for estimating and interpreting SIF across scales. As reviewed in  
78 Mohammed et al.<sup>12</sup> and Aasen et al.<sup>16</sup>, SIF can now be measured from an expanding number of  
79 sensors mounted on towers<sup>17,18</sup>, drones<sup>19,20</sup>, aircraft<sup>21,22</sup> and satellites with ever-improving spatial  
80 and temporal resolution<sup>23,24</sup>. So far, all satellite SIF retrievals have been serendipitous, relying on  
81 instruments originally designed to measure atmospheric gases. The first satellite mission designed  
82 specifically for the measurement of SIF is the ESA FLuorescence EXplorer (FLEX) mission, which  
83 is set to launch in 2024<sup>25</sup>.

84 SIF methods are rapidly breaking through the scale bottleneck of traditional ChlaF measurements,  
85 opening up a range of new opportunities to study photosynthesis across the continuum of spatial  
86 scales from the leaf, through plant canopies, and up to the globe. With SIF we now have the  
87 potential to illuminate the path connecting plant molecular biology to Earth-system science.  
88 However, before the full potential of multiscale SIF observations can be realized, a number of  
89 challenges must be overcome. Extracting the information embedded in the SIF signal requires a  
90 fundamental understanding and a quantitative description of the processes that connect measured  
91 ChlaF with photosynthesis (Fig.1), as well as their variation across space and time (Fig. 2). In this  
92 Perspective, we present these challenges and propose a roadmap of activities to facilitate future  
93 research. Finally, we discuss key emerging SIF applications that can benefit from cross-disciplinary  
94 expertise.

95 **Challenge 1:  $APAR_g$ .** The common denominator between ChlaF and the photosynthetic uptake of  
96 CO<sub>2</sub> is the flux of photosynthetically active radiation absorbed by photosynthetic pigments, or  
97  $APAR_g$  (where the g stands for green), which provides the foundation for the mechanistic  
98 connection between SIF and photosynthesis.  $APAR_g$  is the product of the incoming  
99 photosynthetically active radiation (PAR) and the fraction of this PAR absorbed by photosynthetic  
100 pigments ( $fAPAR_g$ ) (Fig.1). Importantly, although the absorption of radiation by leaves and plant

101 canopies can be quantified using radiometric sensors either coupled to an integrating sphere<sup>26</sup> (e.g.  
102 leaf absorptance profile in Fig.1) or mounted above and below a plant canopy<sup>27</sup>, these  
103 measurements also include a significant and dynamic contribution from non-photosynthetic  
104 pigments and other canopy elements. While inaccuracies in the estimation of APAR<sub>g</sub> do not disrupt  
105 the relationship between SIF and photosynthesis, accurate quantification of the energy flux entering  
106 the photosynthetic process is essential for a mechanistic interpretation of SIF and remains a  
107 challenge.

108 ***Challenge 2: Distribution of excitation energy between PSII and PSI and their ChlaF emissions.***

109 APAR<sub>g</sub> is absorbed mostly by chlorophyll-a and chlorophyll-b associated with either photosystem  
110 II (PSII) or photosystem I (PSI) reaction centres. Interestingly, while both types of chlorophyll have  
111 the capacity to fluoresce, essentially all chlorophyll fluorescence *in vivo* originates from  
112 chlorophyll-a due to the efficient transfer of excitation energy from chlorophyll-b to chlorophyll-a  
113 within light harvesting antennae<sup>28</sup>. Likewise, although both photosystems emit ChlaF, ChlaF from  
114 PSII typically dominates the signal, especially in the red region of the emission spectrum<sup>2</sup> (Fig.1),  
115 and exhibits greater variation in quantum yield in response to photochemical and non-  
116 photochemical processes<sup>7,29</sup>. The dynamic nature of PSII ChlaF explains the widespread application  
117 of PAM fluorescence to probe the energy partitioning between photochemical and non-  
118 photochemical processes or to estimate the rate of linear electron transport (LET) in PSII<sup>30</sup>.  
119 However, the estimation of LET requires knowledge of the distribution of absorption between the  
120 photosystems (i.e. the use of an energy partitioning factor), which is rarely measured and often  
121 assumed to be 0.5<sup>6</sup>. Although biochemical and biophysical methods to assess the stoichiometry and  
122 antenna sizes of PSI and PSII do exist<sup>31-33</sup>, these methods only provide a relative assessment of the  
123 energy distribution; absolute quantification requires the combination of simultaneous ChlaF and  
124 820 nm absorption measurements to probe the energy partitioning in PSII and PSI, respectively,  
125 along with photosynthetic gas exchange measurements<sup>34</sup>. Overall, the evidence gathered to date

126 suggests that neither the distribution of excitation energy between PSII and PSI nor the contribution  
127 of ChlaF from PSI to SIF remain constant over time, between species or within canopy light  
128 gradients<sup>35,36</sup>. Questions remain: how large is this variability? What controls it? And what is its  
129 significance for the interpretation of SIF? Answers to these questions await the development of  
130 versatile field methods and protocols (e.g. based on rapid optical measurements<sup>37</sup>) to enable  
131 the characterization of these factors across a wide range of conditions.

132 **Challenge 3: Energy partitioning in PSII.** Energy absorbed in PSII is partitioned between three  
133 main processes: a) photochemical quenching (PQ) of excitation energy, promoting linear electron  
134 transport, b) non-photochemical quenching (NPQ), which includes both regulated and sustained  
135 forms of thermal dissipation, and c) emission of ChlaF. The quantum yield of a process, e.g. ChlaF  
136 emission ( $\Phi_F$ ), can be expressed as the ratio of the rate constant associated to that process relative  
137 to the sum of all rate constants. Importantly, the rate constants associated to PQ and NPQ are highly  
138 dynamic, which allows plants to regulate the flow of energy through PSII and to protect against  
139 light-induced damage<sup>38,39</sup>. During the growing season, the rate constants of PQ and NPQ vary over  
140 time-scales of seconds to minutes in response to the redox dynamics of the quinone acceptor pool  
141 and induction and relaxation of regulated thermal dissipation, respectively. Outside of the growing  
142 season, or during periods of profound environmental stress, rate constants can be affected by  
143 photoinhibition of PQ and the induction of sustained NPQ. Accordingly, changes in the quantum  
144 yield of ChlaF ( $\Phi_F$ ) reflect the combined effect of PQ and NPQ dynamics and a quantitative  
145 connection between  $\Phi_F$  and  $\Phi_P$  (the quantum yield of photochemistry) cannot be established  
146 without knowledge of either PQ or NPQ<sup>8,40</sup>. PAM fluorescence uses saturating light pulses to solve  
147 the energy partitioning and estimate  $\Phi_P$ ; an approach that is not feasible during SIF measurements,  
148 precluding partitioning from SIF alone.

149 Under certain conditions, either NPQ or PQ can dominate the relationships between  $\Phi_F$  and  $\Phi_P$ ,  
150 resulting in the emergence of a positive or negative relationship respectively. For example, under

151 low light intensities – when regulatory NPQ remains inactive - the relationship between  $\Phi_P$  and  $\Phi_F$   
152 is negative under the action of PQ, which exerts opposite effects on (i.e. decouples)  $\Phi_P$  and  $\Phi_F$ .  
153 Under high light - when PQ tends to saturate and NPQ is highly active - the relationship between  
154  $\Phi_P$  and  $\Phi_F$  turns to positive under the action of NPQ, which competes for excitation with both (i.e.  
155 couples)  $\Phi_P$  and  $\Phi_F$ <sup>12,52,53</sup>. The latter case can explain the seasonal correlation between  $\Phi_P$  and  $\Phi_F$   
156 observed at the leaf<sup>41,42</sup> (Fig. 2) and canopy scales<sup>18</sup>, in response to the modulation of sustained  
157 NPQ that protects the foliage from the harmful combination of excessive light and low  
158 temperatures<sup>43,44</sup>. Despite the positive relationship between  $\Phi_P$  and  $\Phi_F$  that emerges in response to  
159 certain stress conditions, the quantitative treatment of the energy partitioning in PSII requires the  
160 use of mechanistic models and remains one of the core challenges to the interpretation of SIF<sup>40,45,46</sup>.

161 **Challenge 4: Alternative energy sinks.** Photosynthetic linear electron transport provides reducing  
162 power for a range of metabolic processes beyond CO<sub>2</sub> assimilation via the Calvin cycle, including  
163 chlororespiration<sup>47</sup>, photorespiration<sup>48</sup>, nitrogen, sulphur and oxygen reduction (the latter known as  
164 the Mehler reaction in the water-water cycle<sup>49</sup>), and the synthesis of volatile organic compounds<sup>50</sup>.  
165 Importantly, the dynamics of these ‘non-assimilatory’ electron sinks can affect ChlF in a manner  
166 not directly correlated with CO<sub>2</sub> assimilation. In particular, because alternative energy sinks can  
167 have a protective function by sustaining LET under conditions when CO<sub>2</sub> assimilation is impaired<sup>51</sup>,  
168 they could influence the capacity of SIF to detect certain plant stress responses. Therefore, it is  
169 critical to address the extent that these dynamics decouple SIF from GPP, in particular during plant  
170 stress. As with Challenge 2, answering this question will benefit from the development of versatile  
171 field methods and protocols to promote the widespread characterization of these factors across a  
172 wide range of conditions.

173 **Challenge 5: Leaf and canopy ChlF scattering, reabsorption and measurement geometry.**

174 Although the lighter and darker green stripes seen on an athletic field may give the impression of  
175 different chlorophyll contents, they are an optical reflection effect created when the grass is bent in

176 a particular direction during mowing. SIF measurements over plant canopies are similarly affected  
177 by the distribution of leaves, canopy architecture and measurement geometry<sup>27,52</sup>. The amount and  
178 distribution of chlorophyll within a leaf (influenced by photosystem and thylakoid structure,  
179 chloroplast distribution, and internal leaf morphology), as well as the amount and geometrical  
180 arrangement of leaves and other non-photosynthetic material within a plant canopy (influenced by  
181 branch/stem architecture) drive  $APAR_g$ , connecting SIF and photosynthesis at the leaf and canopy  
182 scales, respectively. Once emitted, ChlaF photons travel through the same leaf and canopy  
183 structures, where some of the ChlaF photons are reabsorbed (Fig. 1 and Fig. 2 “spectral dynamics”).  
184 As a result, spatial and temporal variations in leaf biochemistry, leaf morphology, and canopy  
185 architecture, as well as foliage illumination and viewing geometry, influence the probability of  
186 ChlaF photons contributing to a SIF measurement (known as the escape probability). These factors  
187 decouple the total emitted ChlaF from the measured SIF, and by extension from photosynthesis.  
188 Physically-based radiative transfer models, which simulate the movement of photons through leaves  
189 and plant canopies (Box 2), can be used to provide a quantitative framework to investigate and  
190 account for the impact of these factors on  $APAR_g$  and SIF observations<sup>27,53</sup>. Although spatially  
191 explicit RTM approaches are already available (see Supplementary Video 1 and 2), advances in the  
192 parametrization of within-leaf and canopy drivers of SIF - e.g. canopy gradients in foliar  
193 morphology, pigment contents (Challenge 1) or ChlaF contribution from PSI (Challenge 2) - remain  
194 areas of active development.

195 ***Challenge 6: Atmospheric absorption and scattering.*** Atmospheric gases, aerosols and other  
196 particles absorb and scatter ChlaF photons traveling from a plant canopy to a remote detector. The  
197 extent of atmospheric absorption and scattering of SIF depends on the retrieval wavelength, the  
198 distance between target and sensor, and the properties of the atmosphere (Box 1). In particular, SIF  
199 retrieval methods based on the in-filling of atmospheric gas absorption bands, such as the O2-A or  
200 O2-B bands (Fig. 1), face the challenge that the gas absorption feature used for the SIF retrieval

201 simultaneously attenuates the ChlaF signal as it travels towards the detector. This effect requires a  
202 correction even for short-distance measurements from canopy towers and drones<sup>54</sup>. Although an  
203 atmospheric RTM can be used to characterize and correct for these effects, its application requires  
204 site-specific measurements of atmospheric profile parameters for model input, which remains an  
205 operational challenge<sup>55</sup>.

206 ***Challenge 7: Integrating SIF controls across space and time.*** A final challenge, and perhaps the  
207 most relevant, is the contextualization of the interpretation of SIF (including the previous six  
208 challenges) within the spatial and temporal domain of the measurements (Fig. 2). Temporally,  
209 ChlaF dynamics have been used to investigate the energy transfer within photosystems (femto-  
210 picosecond scale)<sup>7,56</sup>, the redox status of the donor and acceptor sides of the photosystem  
211 (microsecond-millisecond scale)<sup>3,4</sup>, and the variations in PQ and NPQ (seconds-to-seasonal scale)<sup>38</sup>.  
212 <sup>39,44</sup>. Spatially, the intensity and spectral properties of SIF are also controlled by factors that regulate  
213 both APAR<sub>g</sub> and ChlaF scattering and reabsorption within a leaf or plant canopy<sup>57,58</sup> (Fig. 2,  
214 “spectral dynamics”). When ChlaF is measured as SIF across coarser spatial and longer temporal  
215 scales, the signal carries information that aggregates an expanding assortment of physical and  
216 biological factors<sup>59-61</sup>. New controls may appear while the effects of others may be subordinated,  
217 strengthening (via ‘couplers’; Fig. 2) or disrupting (via ‘decouplers’; Fig. 2) the relationship  
218 between SIF and GPP.

219 For example, tower-based SIF studies reveal a strong seasonal linear relationship between canopy  
220 SIF and ecosystem GPP across a wide range of ecosystems<sup>17,18,61</sup>, consistent with the coupling  
221 action of APAR<sub>g</sub> and NPQ described above. Yet, the sensitivity, strength and linearity of the  
222 seasonal SIF-GPP relationship is not universal and has been found to depend on additional physical  
223 and physiological decoupling factors, such as sun-vegetation-sensor geometries<sup>62,63</sup>, vegetation  
224 canopy structure<sup>52,64</sup>, or photosynthetic pathway (C3 vs. C4)<sup>27,65</sup>, with contrasting responses to  
225 different environmental stressors<sup>66,67</sup>. Clearly, integrating and disentangling the relationship

226 between SIF and GPP across species, space, time and in response to environmental stress, remains  
227 still a challenge that calls for comprehensive field studies.

## 228 **Roadmap towards a consistent interpretation of SIF**

229 The time for multiscale SIF measurements is already here (Fig. 3). Yet, converting these data into  
230 meaningful information and new applications still requires effort dedicated to scaling and  
231 standardizing methods for SIF interpretation, with particular attention to the seven challenges  
232 described above. This process requires accounting for the influence of 1) instrumental, 2)  
233 atmospheric, 3) structural and 4) physiological factors to unlock the quantitative association  
234 between measured SIF and photosynthesis (Fig. 4). Addressing these challenges requires new data,  
235 protocols and models to interpret SIF and bridge the gap between molecular processes, i.e.  
236 photosynthesis, and satellite imagery.

237 At the leaf level, new instruments and techniques employing optical bandpass filters have been  
238 developed to record fluorescence spectral dynamics under both natural or controlled illumination,  
239 temperature, and CO<sub>2</sub> concentration<sup>16,68-71</sup>. Such spectral approaches, combined with foliar pigment  
240 analysis, photosynthetic gas exchange, and PAM ChlaF measurements, provide new insights into  
241 the connection between SIF and photosynthesis dynamics of leaves<sup>42,69,72</sup>. Going forward,  
242 mechanistically modeling the link between SIF and GPP (**Challenges 1-4**) will require the  
243 combination of field campaigns covering full growing seasons, multiple species and stress  
244 responses with detailed experimentation under highly controlled conditions, for example using  
245 *Arabidopsis* mutants with altered photochemical properties<sup>9,73</sup>. In particular, the development of  
246 versatile field instrumentation and protocols for the estimation of APAR<sub>g</sub> (**Challenge 1**), energy  
247 distribution between PSII and PSI - including the ChlaF contribution from PSI - (**Challenge 2**), or  
248 the quantification of alternative energy sinks (**Challenge 4**), is key to resolving the spatial and  
249 temporal influences of these factors on SIF.

250 The synergistic use of complementary data streams can also help to constrain the modelling of  
251 photosynthesis and support SIF interpretation. For example, leaf and canopy reflectance data can  
252 inform us on the chlorophyll content in the leaf or the amount of leaves in the canopy<sup>74</sup>, relating to  
253  $APAR_g$  (**Challenge 1**). In addition, reflectance data have been used to explore the regulatory  
254 dynamics of NPQ<sup>75</sup>, which could contribute to resolving energy partitioning in PSII (**Challenge 3**).  
255 This approach is feasible due to the spectral change that accompanies the operation of the  
256 xanthophyll cycle<sup>76</sup> - by which violaxanthin is converted to antheraxanthin and zeaxanthin in a  
257 process that modulates NPQ<sup>38,77</sup> - as well as the seasonal dynamics of leaf carotenoid and  
258 chlorophyll contents<sup>78</sup>. These spectral changes, which have been captured by the photochemical  
259 reflectance index (PRI)<sup>77,79</sup> or the Chlorophyll/Carotenoid Index (CCI)<sup>80</sup>, are now being revisited  
260 and investigated in depth across the whole VIS-NIR region alongside with SIF dynamics<sup>71,76</sup>.  
261 Clearly, as in the case of SIF, careful use of canopy and atmospheric RTMs will be needed to  
262 disentangle these subtle physiologically-induced reflectance changes from those of a dynamic  
263 background<sup>55</sup>. In addition to synergies with spectral reflectance, use of thermal imaging<sup>81</sup>, radar<sup>82</sup>,  
264 or multispectral laser scanning methods<sup>83</sup> offer interesting possibilities to constrain the carbon  
265 reactions of photosynthesis by providing independent information on plant water status (**Challenge**  
266 **4**). Likewise, leaf and ecosystem-level measurements of carbonyl sulfide (COS) uptake by  
267 vegetation can provide an independent source of information on stomatal conductance in vascular  
268 plants<sup>84</sup>, which could be highly relevant for the development and validation of ecosystem-level SIF-  
269 GPP models.

270 Process-based and radiative transfer models are required to integrate physical and physiological  
271 mechanisms operating at different scales (**Challenge 7**), providing excellent frameworks for  
272 multidisciplinary collaborations to connect molecular-level with Earth-system processes. Clearly, as  
273 our mechanistic understanding of the connection between SIF and GPP increases (**Challenges 1-4**),  
274 so will the accuracy of process-based models. For example, the integration of the Farquhar-



275 Caemmerer-Berry<sup>85</sup> biochemical model of photosynthesis into dynamic land-surface models (e.g.,  
276 ORCHIDEE<sup>86</sup> or BETHY<sup>87</sup>) provides a gateway for assimilating satellite SIF data and improving  
277 the accuracy of GPP estimations<sup>88,89</sup>. In addition, SIF resides at the core of a new generation of  
278 photosynthesis models that emphasize the light reactions<sup>45,90</sup>. In the case of RTMs with established  
279 SIF capabilities (Box 2), further improvements can be achieved by coupling with new techniques  
280 measuring detailed 3D structures. Leaf RTMs would benefit from including variations in leaf  
281 morphology, thylakoid structure, or the spectral signatures of PSI and PSII. The 3D  
282 parameterization of canopy RTMs via lidar-based reconstruction methods<sup>91,92</sup>, coupled to non-  
283 imaging<sup>17,19</sup> and imaging proximal/airborne SIF measurements (Fig. 3)<sup>93,94</sup>, offers excellent  
284 opportunities to integrate and resolve the diversity of factors that control SIF across space and time  
285 (**Challenge 7**). Drone-based measurements could serve to investigate and model the impact of  
286 atmospheric properties on SIF retrieval approaches, by hovering at different distances above the  
287 target<sup>54</sup> (**Challenge 6**). Finally, less accurate but simpler alternative methods for separating the  
288 physiological and structural influences on the SIF signal have been recently proposed based on the  
289 theory of vegetation canopy near-infrared spectral invariants<sup>95,96</sup>. Whether this or other correction  
290 methods are applicable to canopy SIF acquisitions across scales, especially observations at very  
291 high spatial resolutions (Fig. 3) should be further investigated.

292 Equally critical for the consistent interpretation of SIF is the establishment of a global network and  
293 database of leaf and ecosystem-level SIF measurements covering different biomes, and supporting  
294 model development as well as airborne and satellite calibration/validation activities. While regional  
295 SIF networks are starting to emerge in North America, Europe, and Asia, their global connectivity  
296 should be a priority to promote the adoption of standards for instrument calibrations and long-term  
297 monitoring operations (Fig. 4).

298 Our roadmap for resolving the seven SIF challenges will only succeed through multidisciplinary  
299 collaboration involving specialists from across molecular biology, plant physiology, optical physics

300 and remote sensing. Together, the characterization and modeling of the interplay between structural,  
301 optical and functional dynamics of leaves and plant canopies, can turn our crops and forests into  
302 observable field laboratories.

### 303 **Emerging and potential SIF applications**

304 Satellite SIF data are already providing new insight into photosynthetic dynamics at the global  
305 scale<sup>97,98</sup>. Likewise, with the advent of multiscale SIF measurements (Fig. 3), and as the remaining  
306 challenges are overcome (Fig. 4), a new range of SIF applications unfolds across fields of  
307 biochemistry, biophysics, ecology, ecophysiology, biogeochemistry, agriculture and forestry (Fig.  
308 5). Equally important, the continuum of scales at which SIF can be measured provides a focal point  
309 to promote and strengthen the interaction between research communities, from plant molecular  
310 biology to Earth-system science. Here, we outline four examples of potential and emerging SIF  
311 applications.

312 ***Spatial and 3D photosynthesis.*** Photosynthetic CO<sub>2</sub> assimilation can be measured using infrared  
313 gas analyzers, either coupled to chambers or enclosures at the leaf, shoot, and whole-plant level<sup>99</sup>,  
314 or with a sonic anemometer at the ecosystem level using the eddy covariance approach<sup>100</sup>. These  
315 methods, however, lack detailed spatial information. Spatial measurements of photosynthesis, in  
316 terms of photochemical rates of the light reactions, require the use of imaging systems that, to date,  
317 have remained restricted to the scale of leaves or small-sized plants, e.g. PAM imaging methods<sup>101</sup>.  
318 SIF measurements have potential to fill this scale gap. For example, SIF imaging (Fig. 3) could be  
319 benchmarked with eddy-covariance methods to reveal the spatial variability of photosynthesis  
320 within the footprint of ecosystem eddy covariance measurements, allowing us to investigate the  
321 influence of microenvironment, understory and vertical canopy structure, or the interplay between  
322 biological and functional diversity within the ecosystem. Likewise, SIF imaging could be applied to

323 resolve photosynthesis dynamics in 3D, helping to advance our understanding of the interaction  
324 between plant structure and function<sup>102,103</sup>.

325 ***Physiological phenotyping and pre-visual stress detection.*** Spatial and temporal variations in plant  
326 morphological traits (e.g., canopy height, leaf area, and plant growth) have been widely used as  
327 markers for field phenotypic variability and to investigate long-term plant stress responses.  
328 However, these traits are insufficiently responsive to rapid plant physiological changes. This makes  
329 them ill-suited for physiological phenotyping (i.e. breeding plant phenotypes displaying specific  
330 physiological responses to the environment), or pre-visual stress detection and subsequent  
331 optimization of water, pesticide and fertilizer use. The current phenotyping focus has, therefore,  
332 shifted towards measurements in the visible and infrared spectral ranges, where reflectance changes  
333 can be associated with specific physiological and biochemical traits<sup>104</sup> or used for early-stress  
334 detection<sup>105</sup>. In this context, emerging SIF imaging systems have already provided promising results  
335 for applications in precision agriculture and detection of pest infestations<sup>93,106</sup>. In the near future,  
336 these methods could also support precision forestry applications related to seedling production or  
337 tree-scale forest management.

338 ***Functional plant diversity and spatial ecology.*** Functional diversity is a fundamental component of  
339 the biodiversity concept<sup>107</sup>. As a global network for monitoring biodiversity through remotely  
340 sensed plant functional traits is being developed<sup>108</sup>, SIF could become one of the new essential  
341 variables for mapping functional diversity across ecosystem and landscape scales, given the wide  
342 range of biochemical and physiological factors that SIF is sensitive to (Fig. 2) in relation to plant  
343 productivity. For example, SIF has been shown to convey spatial information on leaf mass and  
344 chlorophyll content<sup>109</sup>, and other functional plant traits<sup>110</sup> in various forest ecosystems. Additionally  
345 and importantly, the combination of high-resolution structural, spectral and SIF data is potentially  
346 the only viable option to investigate ecosystem functions that have remained hidden from our  
347 observational abilities, such as photosynthetic phenology in evergreen forests<sup>18</sup>, cryptogamic

348 biocrusts<sup>111</sup> and spatially fragmented Antarctic mosses<sup>74</sup>. Together with spatial photosynthesis, SIF  
349 could also offer unique opportunities for studies in spatial ecology<sup>111,112</sup>, where plant environmental  
350 responses and biotic interactions could leave their imprint on SIF.

351 ***Carbon and water cycle studies.*** The carbon and water cycles of terrestrial ecosystems are  
352 intricately connected via stomatal regulation and total leaf area. Because both canopy  
353 evapotranspiration and canopy SIF dynamics are strongly controlled by leaf area, and since ChlaF  
354 can also decrease with stomatal closure - via increased NPQ in response to water stress<sup>113, 114</sup>; tower  
355 and satellite SIF have been preliminarily used to investigate canopy conductance and plant  
356 transpiration<sup>115,116</sup>. No doubt, better constraints on transpiration and photosynthetic dynamics in  
357 land-surface models will be achieved as the mechanistic basis of SIF is elucidated across scales  
358 (Challenges 1-7), and the integration of SIF with other remote sensing datasets increases, such as  
359 land-surface temperature<sup>115</sup>, surface soil moisture<sup>89</sup>, radar-measured vegetation optical depth  
360 characterizing canopy structure and water content<sup>117</sup>, or column-averaged atmospheric CO<sub>2</sub><sup>92</sup>. New  
361 knowledge of photosynthesis at the ecosystem and regional scales will bring further insight into the  
362 large-scale interactions between environmental drivers and plant productivity, and feedbacks  
363 between the biosphere and atmosphere.

## 364 **Concluding remarks**

365 The SIF signal gathers a wealth of physiological, biochemical, and structural information as it  
366 travels from the photosystems to the top of canopy and beyond (Fig. 2). This can leave the  
367 impression that SIF is, to use the classic analogy, the ‘Swiss Army Knife’ of photosynthesis  
368 measurements. Critically, the variation in SIF caused by physical and biotic factors is entangled in  
369 the spatiotemporal domain, and our capacity to disentangle it into useful informative components  
370 requires further attention. Historically, photosynthesis research has been a multidisciplinary  
371 endeavor, with breakthroughs in the 20<sup>th</sup> century emerging from collaboration between chemists,

372 biologists and physicists. We are now entering a new era of multiscale observations of  
373 photosynthesis which requires the interdisciplinary research environment to flourish further, this  
374 time to resolve the mechanistic connection between SIF and GPP and to scale it across space and  
375 time. The technology to measure SIF is developing at a faster pace than our capacity to interpret the  
376 acquired data. With the challenges, roadmap and unfolding opportunities introduced here we hope  
377 to encourage more scientists to join the multidisciplinary quest to reveal the true potential of SIF  
378 observation.

379

## 380 **References**

- 381 1. Genty, B., Wonders, J. & Baker, N. R. Non-photochemical quenching of Fo in leaves is  
382 emission wavelength dependent: consequences for quenching analysis and its interpretation.  
383 *Photosynth. Res.* **26**, 133-139 (1990).
- 384 2. Franck, F., Juneau, P. & Popovic, R. Resolution of the photosystem I and photosystem II  
385 contributions to chlorophyll fluorescence of intact leaves at room temperature. *Biochim.*  
386 *Biophys. Acta-Bioenergetics* **1556**, 239-246 (2002).
- 387 3. Neubauer, C. & Schreiber, U. The polyphasic rise of chlorophyll fluorescence upon onset of  
388 strong continuous illumination: I. Saturation characteristics and partial control by the  
389 photosystem II acceptor side. *Zeitschrift für Naturforschung C* **42**, 1246-1254 (1987).
- 390 4. Strasser, R. J., Tsimilli-Michael, M. & Srivastava, A. Analysis of the chlorophyll a  
391 fluorescence transient. In: Papageorgiou G.C., Govindjee (eds) Chlorophyll a Fluorescence.  
392 Advances in Photosynthesis and Respiration, vol 19. Springer, Dordrecht (2004).
- 393 5. Schreiber, U., Schliwa, U. & Bilger, W. Continuous recording of photochemical and non-  
394 photochemical chlorophyll fluorescence quenching with a new type of modulation  
395 fluorometer. *Photosynth. Res.* **10**, 51-62 (1986).

- 396 6. Maxwell, K. & Johnson, G. N. Chlorophyll fluorescence—a practical guide. *J. Exp. Bot.* **51**,  
397 659-668 (2000).
- 398 7. Govindjee, E. 63 Years since Kautsky-chlorophyll-a fluorescence. *Aust. J. Plant Physiol.* **22**,  
399 131-160 (1995).
- 400 8. Porcar-Castell, A. *et al.* Linking chlorophyll a fluorescence to photosynthesis for remote  
401 sensing applications: mechanisms and challenges. *J. Exp. Bot.* **65**, 4065-4095 (2014).
- 402 9. Tikkanen, M., Rantala, S., Grieco, M. & Aro, E. Comparative analysis of mutant plants  
403 impaired in the main regulatory mechanisms of photosynthetic light reactions-From  
404 biophysical measurements to molecular mechanisms. *Plant Physiol. Biochem.* **112**, 290-301  
405 (2017).
- 406 10. Kolber, Z. *et al.* Measuring photosynthetic parameters at a distance: laser induced  
407 fluorescence transient (LIFT) method for remote measurements of photosynthesis in  
408 terrestrial vegetation. *Photosynth. Res.* **84**, 121-129 (2005).
- 409 11. Keller, B. *et al.* Genotype specific photosynthesis x environment interactions captured by  
410 automated fluorescence canopy scans over two fluctuating growing seasons. *Front. Plant*  
411 *Sci.* **10**, 1482 (2019).
- 412 12. Mohammed, G. H. *et al.* Remote sensing of solar-induced chlorophyll fluorescence (SIF) in  
413 vegetation: 50 years of progress. *Remote Sens. Environ.* **231**, 111177 (2019).
- 414 13. Evain, S., Camenen, L. & Moya, I. Three-channel detector for remote sensing of chlorophyll  
415 fluorescence and reflectance from vegetation. In: M. Leroy (ed.), 8<sup>th</sup> International  
416 symposium: physical measurements and signatures in remote sensing, pp. 395-400. Aussois,  
417 CNES, France (2001).
- 418 14. Louis, J. *et al.* Remote sensing of sunlight-induced chlorophyll fluorescence and reflectance  
419 of Scots pine in the boreal forest during spring recovery. *Remote Sens. Environ.* **96**, 37-48  
420 (2005).

- 421 15. Guanter, L. *et al.* Estimation of solar-induced vegetation fluorescence from space  
422 measurements. *Geophys. Res. Lett.* **34** (2007).
- 423 16. Aasen, H. *et al.* Sun-induced chlorophyll fluorescence II: review of passive measurement  
424 setups, protocols, and their application at the leaf to canopy level. *Remote Sensing* **11**, 927  
425 (2019).
- 426 17. Yang, X. *et al.* Solar-induced chlorophyll fluorescence that correlates with canopy  
427 photosynthesis on diurnal and seasonal scales in a temperate deciduous forest. *Geophys.*  
428 *Res. Lett.* **42**, 2977-2987 (2015).
- 429 18. Magney, T. S. *et al.* Mechanistic evidence for tracking the seasonality of photosynthesis  
430 with solar-induced fluorescence. *PNAS* **116**, 11640-11645 (2019).
- 431 19. Bendig, J., Malenovský, Z., Gautam, D. & Lucieer, A. Solar-Induced Chlorophyll  
432 Fluorescence Measured From an Unmanned Aircraft System: Sensor Etaloning and Platform  
433 Motion Correction. *IEEE Trans. Geosci. Remote Sens.* (2019).
- 434 20. Vargas, J. Q. *et al.* Unmanned aerial systems (UAS)-based methods for solar induced  
435 chlorophyll fluorescence (SIF) retrieval with non-imaging spectrometers: state of the art.  
436 *Remote Sens.* **12**, 1624 (2020).
- 437 21. Rascher, U. *et al.* Sun-induced fluorescence—a new probe of photosynthesis: First maps from  
438 the imaging spectrometer HyPlant. *Global Change Biol.* **21**, 4673-4684 (2015).
- 439 22. Frankenberg, C. *et al.* The Chlorophyll Fluorescence Imaging Spectrometer (CFIS),  
440 mapping far red fluorescence from aircraft. *Remote Sens. Environ.* **217**, 523-536 (2018).
- 441 23. Frankenberg, C. *et al.* New global observations of the terrestrial carbon cycle from GOSAT:  
442 Patterns of plant fluorescence with gross primary productivity. *Geophys. Res. Lett.* **38**  
443 (2011).
- 444 24. Köhler, P. *et al.* Global Retrievals of Solar-Induced Chlorophyll Fluorescence at Red  
445 Wavelengths With TROPOMI. *Geophys. Res. Lett.* **47**, e2020GL087541 (2020).

- 446 25. Drusch, M. *et al.* The fluorescence explorer mission concept - ESA's earth explorer 8. *IEEE*  
447 *Trans. Geosci. Remote Sens.* **55**, 1273-1284 (2016).
- 448 26. Olascoaga, B., Mac Arthur, A., Atherton, J. & Porcar-Castell, A. A comparison of methods  
449 to estimate photosynthetic light absorption in leaves with contrasting morphology. *Tree*  
450 *Physiol.* **36**, 368-379 (2016).
- 451 27. Zhang, Z. *et al.* Assessing bi-directional effects on the diurnal cycle of measured solar-  
452 induced chlorophyll fluorescence in crop canopies. *Agric. For. Meteorol.* **295**, 108147  
453 (2020).
- 454 28. Bittner, T., Irrgang, K., Renger, G. & Wasielewski, M. R. Ultrafast excitation energy  
455 transfer and exciton-exciton annihilation processes in isolated light harvesting complexes of  
456 photosystem II (LHC II) from spinach. *J. Phys. Chem.* **98**, 11821-11826 (1994).
- 457 29. Kalaji, H. M. *et al.* Frequently asked questions about chlorophyll fluorescence, the sequel.  
458 *Photosynth. Res.* **132**, 13-66 (2017).
- 459 30. Genty, B., Briantais, J. & Baker, N. R. The relationship between the quantum yield of  
460 photosynthetic electron transport and quenching of chlorophyll fluorescence. *Biochim.*  
461 *Biophys. Acta-General Subjects* **990**, 87-92 (1989).
- 462 31. Anderson, J. M., Chow, W. S. & Goodchild, D. J. Thylakoid membrane organisation in  
463 sun/shade acclimation. *Funct. Plant Biol.* **15**, 11-26 (1988).
- 464 32. Ballottari, M., Dall'Osto, L., Morosinotto, T. & Bassi, R. Contrasting behavior of higher  
465 plant photosystem I and II antenna systems during acclimation. *J. Biol. Chem.* **282**, 8947-  
466 8958 (2007).
- 467 33. Schreiber, U., Klughammer, C. & Kolbowski, J. Assessment of wavelength-dependent  
468 parameters of photosynthetic electron transport with a new type of multi-color PAM  
469 chlorophyll fluorometer. *Photosynth. Res.* **113**, 127-144 (2012).



- 470 34. Laisk, A. *et al.* A computer-operated routine of gas exchange and optical measurements to  
471 diagnose photosynthetic apparatus in leaves. *Plant, Cell Environ.* **25**, 923-943 (2002).
- 472 35. Pfündel, E. Estimating the contribution of photosystem I to total leaf chlorophyll  
473 fluorescence. *Photosynthesis Res.* **56**, 185-195 (1998).
- 474 36. Peterson, R. B. *et al.* Fluorescence Fo of photosystems II and I in developing C3 and C4  
475 leaves, and implications on regulation of excitation balance. *Photosynth. Res.* **122**, 41-56
- 476 37. Pfündel, E. E. Simultaneously measuring pulse-amplitude-modulated (PAM) chlorophyll  
477 fluorescence of leaves at wavelengths shorter and longer than 700 nm. *Photosynth. Res.*, 1-  
478 14 (2021).
- 479 38. Demmig-Adams, B. & Adams III, W. W. Photoprotection in an ecological context: the  
480 remarkable complexity of thermal energy dissipation. *New Phytol.* **172**, 11-21 (2006).
- 481 39. Porcar-Castell, A. A high-resolution portrait of the annual dynamics of photochemical and  
482 non-photochemical quenching in needles of *Pinus sylvestris*. *Physiol. Plant.* **143**, 139-153  
483 (2011).
- 484 40. Van der Tol, C., Berry, J. A., Campbell, P. & Rascher, U. Models of fluorescence and  
485 photosynthesis for interpreting measurements of solar-induced chlorophyll fluorescence. *J.*  
486 *Geophys. Res.: Biogeosciences* **119**, 2312-2327 (2014).
- 487 41. Springer, K. R., Wang, R. & Gamon, J. A. Parallel seasonal patterns of photosynthesis,  
488 fluorescence, and reflectance indices in boreal trees. *Remote Sens.* **9**, 691 (2017).
- 489 42. Zhang, C. *et al.* Do all chlorophyll fluorescence emission wavelengths capture the spring  
490 recovery of photosynthesis in boreal evergreen foliage? *Plant, Cell Environ.* **42**, 3264-3279  
491 (2019).
- 492 43. Ensminger, I. *et al.* Intermittent low temperatures constrain spring recovery of  
493 photosynthesis in boreal Scots pine forests. *Glob. Change Biol.* **10**, 995-1008 (2004).

- 494 44. Verhoeven, A. Sustained energy dissipation in winter evergreens. *New Phytol.* **201**, 57-65  
495 (2014).
- 496 45. Gu, L., Han, J., Wood, J. D., Chang, C. Y. & Sun, Y. Sun-induced Chl fluorescence and its  
497 importance for biophysical modeling of photosynthesis based on light reactions. *New*  
498 *Phytol.* **223**, 1179-1191 (2019).
- 499 46. Raczka, B. *et al.* Sustained nonphotochemical quenching shapes the seasonal pattern of  
500 solar-induced fluorescence at a high-elevation evergreen forest. *J. Geophys. Res.:  
501 Biogeosciences* **124**, 2005-2020 (2019).
- 502 47. Nixon, P. J. Chlororespiration. *Philos. Trans. R. Soc. Lond., B, Biol. Sci.* **355**, 1541-1547  
503 (2000).
- 504 48. Ogren, W. L. Photorespiration: pathways, regulation, and modification. *Annu. Rev. Plant*  
505 *Physiol.* **35**, 415-442 (1984).
- 506 49. Asada, K. The water-water cycle in chloroplasts: scavenging of active oxygens and  
507 dissipation of excess photons. *Annu. Rev. Plant Biol.* **50**, 601-639 (1999).
- 508 50. Morfopoulos, C. *et al.* A model of plant isoprene emission based on available reducing  
509 power captures responses to atmospheric CO<sub>2</sub>. *New Phytol.* **203**, 125-139 (2014).
- 510 51. Maseyk, K., Lin, T., Cochavi, A., Schwartz, A. & Yakir, D. Quantification of leaf-scale  
511 light energy allocation and photoprotection processes in a Mediterranean pine forest under  
512 extensive seasonal drought. *Tree Physiol.* **39**, 1767-1782 (2019).
- 513 52. Migliavacca, M. *et al.* Plant functional traits and canopy structure control the relationship  
514 between photosynthetic CO<sub>2</sub> uptake and far-red sun-induced fluorescence in a Mediterranean  
515 grassland under different nutrient availability. *New Phytol.* **214**, 1078-1091 (2017).
- 516 53. Kallel, A. FluLCVRT: Reflectance and fluorescence of leaf and canopy modeling based on  
517 Monte Carlo vector radiative transfer simulation. *J. Quant. Spectrosc. Radiat. Transf.* **253**,  
518 107183 (2020).

- 519 54. Sabater, N. *et al.* Compensation of oxygen transmittance effects for proximal sensing  
520 retrieval of canopy-leaving sun-induced chlorophyll fluorescence. *Remote Sens.* **10**, 1551  
521 (2018).
- 522 55. Sabater, N., Kolmonen, P., Van Wittenberghe, S., Arola, A. & Moreno, J. Challenges in the  
523 atmospheric characterization for the retrieval of spectrally resolved fluorescence and PRI  
524 region dynamics from space. *Remote Sens. Environ.* **254**, 112226 (2021).
- 525 56. Iermak, I., Vink, J., Bader, A. N., Wientjes, E. & van Amerongen, H. Visualizing  
526 heterogeneity of photosynthetic properties of plant leaves with two-photon fluorescence  
527 lifetime imaging microscopy. *Biochim. Biophys. Acta-Bioenergetics* **1857**, 1473-1478  
528 (2016).
- 529 57. Romero, J. M., Cordon, G. B. & Lagorio, M. G. Modeling re-absorption of fluorescence  
530 from the leaf to the canopy level. *Remote Sens. Environ.* **204**, 138-146 (2018).
- 531 58. Magney, T. S. *et al.* Disentangling changes in the spectral shape of chlorophyll  
532 fluorescence: Implications for remote sensing of photosynthesis. *J. Geophys. Res.:  
533 Biogeosciences* **124**, 1491-1507 (2019).
- 534 59. Murchie, E. H. *et al.* Measuring the dynamic photosynthome. *Ann. Bot.* **122**, 207-220  
535 (2018).
- 536 60. Magney, T. S., Barnes, M. L. & Yang, X. On the covariation of chlorophyll fluorescence  
537 and photosynthesis across scales. *Geophys. Res. Lett.* **47**, e2020GL091098 (2020).
- 538 61. Yang, P., van der Tol, C., Campbell, P. K. & Middleton, E. M. Unraveling the physical and  
539 physiological basis for the solar-induced chlorophyll fluorescence and photosynthesis  
540 relationship using continuous leaf and canopy measurements of a corn crop. *Biogeosciences*  
541 **18**, 441-465 (2021).
- 542 62. Liu, X. *et al.* Downscaling of solar-induced chlorophyll fluorescence from canopy level to  
543 photosystem level using a random forest model. *Remote Sens. Environ.* **231**, 110772 (2019).

- 544 63. Joiner, J. *et al.* Systematic Orbital Geometry-Dependent Variations in Satellite Solar-  
545 Induced Fluorescence (SIF) Retrievals. *Remote Sens.* **12**, 2346 (2020).
- 546 64. Dechant, B. *et al.* Canopy structure explains the relationship between photosynthesis and  
547 sun-induced chlorophyll fluorescence in crops. *Remote Sens. Environ.* **241**, 111733 (2020).
- 548 65. He, L. *et al.* From the Ground to Space: Using Solar-Induced Chlorophyll Fluorescence to  
549 Estimate Crop Productivity. *Geophys. Res. Lett.* **47**, e2020GL087474 (2020).
- 550 66. Ač, A. *et al.* Meta-analysis assessing potential of steady-state chlorophyll fluorescence for  
551 remote sensing detection of plant water, temperature and nitrogen stress. *Remote Sens.*  
552 *Environ.* **168**, 420-436 (2015).
- 553 67. Wohlfahrt, G. *et al.* Sun-induced fluorescence and gross primary productivity during a heat  
554 wave. *Sci. Rep.* **8**, 1-9 (2018).
- 555 68. Van Wittenberghe, S., Alonso, L., Verrelst, J., Moreno, J. & Samson, R. Bidirectional sun-  
556 induced chlorophyll fluorescence emission is influenced by leaf structure and light  
557 scattering properties: A bottom-up approach. *Remote Sens. Environ.* **158**, 169-179 (2015).
- 558 69. Magney, T. S. *et al.* Connecting active to passive fluorescence with photosynthesis: A  
559 method for evaluating remote sensing measurements of Chl fluorescence. *New Phytol.* **215**,  
560 1594-1608 (2017).
- 561 70. Rajewicz, P. A., Atherton, J., Alonso, L. & Porcar-Castell, A. Leaf-level spectral  
562 fluorescence measurements: comparing methodologies for broadleaves and needles. *Remote*  
563 *Sens.* **11**, 532 (2019).
- 564 71. Van Wittenberghe, S., Alonso, L., Malenovský, Z. & Moreno, J. In vivo photoprotection  
565 mechanisms observed from leaf spectral absorbance changes showing VIS-NIR slow-  
566 induced conformational pigment bed changes. *Photosynth. Res.* **142**, 283-305 (2019).

- 567 72. Meeker, E. W., Magney, T. S., Bamburg, N., Momayyezi, M. & McElrone, A. J.  
568 Modification of a gas exchange system to measure active and passive chlorophyll  
569 fluorescence simultaneously under field conditions. *AoB Plants* **13**, plaa066 (2021).
- 570 73. Acebron, K. *et al.* Diurnal dynamics of nonphotochemical quenching in *Arabidopsis npq*  
571 mutants assessed by solar-induced fluorescence and reflectance measurements in the field.  
572 *New Phytol.* (2020).
- 573 74. Malenovský, Z., Lucieer, A., King, D. H., Turnbull, J. D. & Robinson, S. A. Unmanned  
574 aircraft system advances health mapping of fragile polar vegetation. *Methods Ecol. Evol.* **8**,  
575 1842-1857 (2017).
- 576 75. Atherton, J., Nichol, C. J. & Porcar-Castell, A. Using spectral chlorophyll fluorescence and  
577 the photochemical reflectance index to predict physiological dynamics. *Remote Sens.*  
578 *Environ.* **176**, 17-30 (2016).
- 579 76. Van Wittenberghe, S. *et al.* Combined dynamics of the 500–600 nm leaf absorption and  
580 chlorophyll fluorescence changes in vivo: Evidence for the multifunctional energy  
581 quenching role of xanthophylls. *Biochim. Biophys. Acta-Bioenergetics* **1862**, 148351 (2021).
- 582 77. Gamon, J. A. *et al.* Remote sensing of the xanthophyll cycle and chlorophyll fluorescence in  
583 sunflower leaves and canopies. *Oecologia* **85**, 1-7 (1990).
- 584 78. Filella, I. *et al.* PRI assessment of long-term changes in carotenoids/chlorophyll ratio and  
585 short-term changes in de-epoxidation state of the xanthophyll cycle. *Int. J. Remote Sens.* **30**,  
586 4443-4455 (2009).
- 587 79. Peñuelas, J., Filella, I. & Gamon, J. A. Assessment of photosynthetic radiation-use  
588 efficiency with spectral reflectance. *New Phytol.* **131**, 291-296 (1995).
- 589 80. Gamon, J. A. *et al.* A remotely sensed pigment index reveals photosynthetic phenology in  
590 evergreen conifers. *PNAS* **113**, 13087-13092 (2016).

- 591 81. Costa, J. M., Grant, O. M. & Chaves, M. M. Thermography to explore plant-environment  
592 interactions. *J. Exp. Bot.* **64**, 3937-3949 (2013).
- 593 82. Konings, A. G., Rao, K. & Steele-Dunne, S. C. Macro to micro: microwave remote sensing  
594 of plant water content for physiology and ecology. *New Phytol.* **223**, 1166-1172 (2019).
- 595 83. Junttila, S. *et al.* Terrestrial laser scanning intensity captures diurnal variation in leaf water  
596 potential. *Remote Sens. Environ.* **255**, 112274 (2021).
- 597 84. Whelan, M. E. *et al.* Two Scientific Communities Striving for a Common Cause:  
598 innovations in carbon cycle science. *Bull. Am. Meteorol. Soc.* (2020).
- 599 85. Farquhar, G. D., von Caemmerer, S. v. & Berry, J. A. A biochemical model of  
600 photosynthetic CO<sub>2</sub> assimilation in leaves of C<sub>3</sub> species. *Planta* **149**, 78-90 (1980).
- 601 86. Bacour, C. *et al.* Improving estimates of gross primary productivity by assimilating solar-  
602 induced fluorescence satellite retrievals in a terrestrial biosphere model using a process-  
603 based SIF model. *J. Geophys. Res.: Biogeosciences* **124**, 3281-3306 (2019).
- 604 87. Norton, A. J. *et al.* Estimating global gross primary productivity using chlorophyll  
605 fluorescence and a data assimilation system with the BETHY-SCOPE model.  
606 *Biogeosciences* **16**, 3069-3093 (2019).
- 607 88. Thum, T. *et al.* Modelling sun-induced fluorescence and photosynthesis with a land surface  
608 model at local and regional scales in northern Europe. *Biogeosciences* **14**, 1969-1987  
609 (2017).
- 610 89. Qiu, B., Chen, J. M., Ju, W., Zhang, Q. & Zhang, Y. Simulating emission and scattering of  
611 solar-induced chlorophyll fluorescence at far-red band in global vegetation with different  
612 canopy structures. *Remote Sens. Environ.* **233**, 111373 (2019).
- 613 90. Johnson, J. E. & Berry, J. A. The role of Cytochrome b<sub>6</sub>f in the control of steady-state  
614 photosynthesis: a conceptual and quantitative model. *Photosynth. Res.*, 1-36 (2021).

- 615 91. Janoutová, R. *et al.* Influence of 3D spruce tree representation on accuracy of airborne and  
616 satellite forest reflectance simulated in DART. *Forests* **10**, 292 (2019).
- 617 92. Liu, W. *et al.* Simulating solar-induced chlorophyll fluorescence in a boreal forest stand  
618 reconstructed from terrestrial laser scanning measurements. *Remote Sens. Environ.* **232**,  
619 111274 (2019).
- 620 93. Pinto, F. *et al.* Sun-induced chlorophyll fluorescence from high-resolution imaging  
621 spectroscopy data to quantify spatio-temporal patterns of photosynthetic function in crop  
622 canopies. *Plant, Cell Environ.* **39**, 1500-1512 (2016).
- 623 94. Siegmann, B. *et al.* The high-performance airborne imaging spectrometer HyPlant—From  
624 raw images to top-of-canopy reflectance and fluorescence products: Introduction of an  
625 automatized processing chain. *Remote Sens.* **11**, 2760 (2019).
- 626 95. Yang, P., van der Tol, C., Campbell, P. K. & Middleton, E. M. Fluorescence Correction  
627 Vegetation Index (FCVI): A physically based reflectance index to separate physiological  
628 and non-physiological information in far-red sun-induced chlorophyll fluorescence. *Remote*  
629 *Sens. Environ.* **240**, 111676 (2020).
- 630 96. Zeng, Y. *et al.* A radiative transfer model for solar induced fluorescence using spectral  
631 invariants theory. *Remote Sens. Environ.* **240**, 111678 (2020).
- 632 97. Green, J. K. *et al.* Large influence of soil moisture on long-term terrestrial carbon uptake.  
633 *Nature* **565**, 476 (2019).
- 634 98. Wang, S. *et al.* Urban– rural gradients reveal joint control of elevated CO<sub>2</sub> and temperature  
635 on extended photosynthetic seasons. *Nat. Ecol. Evo.* **3**, 1076-1085 (2019).
- 636 99. Long, S. P., Farage, P. K. & Garcia, R. L. Measurement of leaf and canopy photosynthetic  
637 CO<sub>2</sub> exchange in the field. *J. Exp. Bot.* **47**, 1629-1642 (1996).

- 638 100. Baldocchi, D. D. Assessing the eddy covariance technique for evaluating carbon dioxide  
639 exchange rates of ecosystems: past, present and future. *Glob. Change Biol.* **9**, 479-492  
640 (2003).
- 641 101. Kaiser, Y. I., Menegat, A. & Gerhards, R. Chlorophyll fluorescence imaging: a new method  
642 for rapid detection of herbicide resistance in *Alopecurus myosuroides*. *Weed Res.* **53**, 399-  
643 406 (2013).
- 644 102. Sievänen, R., Godin, C., DeJong, T. M. & Nikinmaa, E. Functional–structural plant models:  
645 a growing paradigm for plant studies. *Ann. Bot.* **114**, 599-603 (2014).
- 646 103. Damm, A., Paul-Limoges, E., Kükenbrink, D., Bachofen, C. & Morsdorf, F. Remote sensing  
647 of forest gas exchange: Considerations derived from a tomographic perspective. *Glob.*  
648 *Change Biol.* **26**, 2717-2727 (2020).
- 649 104. Ensminger, I. Fast track diagnostics: Hyperspectral reflectance differentiates disease from  
650 drought stress in trees. *Tree Physiol.* **40**, 1143-1146 (2020).
- 651 105. Mutka, A. M. & Bart, R. S. Image-based phenotyping of plant disease symptoms. *Frontiers*  
652 *in plant science* **5**, 734 (2015).
- 653 106. Zarco-Tejada, P. J. *et al.* Previsual symptoms of *Xylella fastidiosa* infection revealed in  
654 spectral plant-trait alterations. *Nat. Plants* **4**, 432-439 (2018).
- 655 107. Díaz, S. & Cabido, M. Vive la différence: plant functional diversity matters to ecosystem  
656 processes. *Trends Ecol. Evol.* **16**, 646-655 (2001).
- 657 108. Skidmore, A. K. *et al.* Environmental science: Agree on biodiversity metrics to track from  
658 space. *Nat. News* **523**, 403 (2015).
- 659 109. Tagliabue, G. *et al.* Sun–induced fluorescence heterogeneity as a measure of functional  
660 diversity. *Remote Sens. Environ.* **247**, 111934 (2020).



- 661 110. Pacheco-Labrador, J. *et al.* Multiple-constraint inversion of SCOPE. Evaluating the potential  
662 of GPP and SIF for the retrieval of plant functional traits. *Remote Sens. Environ.* **234**,  
663 111362 (2019).
- 664 111. Smith, W. K. *et al.* Remote sensing of dryland ecosystem structure and function: Progress,  
665 challenges, and opportunities. *Remote Sens. Environ.* **233**, 111401 (2019).
- 666 112. Kellner, J. R., Albert, L. P., Burley, J. T. & Cushman, K. C. The case for remote sensing of  
667 individual plants. *Am. J. Bot.* **106**, 1139-1142 (2019).
- 668 113. Flexas, J. *et al.* Steady-state chlorophyll fluorescence (Fs) measurements as a tool to follow  
669 variations of net CO<sub>2</sub> assimilation and stomatal conductance during water-stress in C<sub>3</sub>  
670 plants. *Physiol. Plant.* **114**, 231-240 (2002).
- 671 114. Marrs, J. K. *et al.* Solar-induced fluorescence does not track photosynthetic carbon  
672 assimilation following induced stomatal closure. *Geophys. Res. Lett.* **47**, e2020GL087956  
673 (2020).
- 674 115. Maes, W. H. *et al.* Sun-induced fluorescence closely linked to ecosystem transpiration as  
675 evidenced by satellite data and radiative transfer models. *Remote Sens. Environ.* **249**,  
676 112030 (2020).
- 677 116. Shan, N. *et al.* A model for estimating transpiration from remotely sensed solar-induced  
678 chlorophyll fluorescence. *Remote Sens. Environ.* **252**, 112134 (2021).
- 679 117. Liu, W. *et al.* Simulating solar-induced chlorophyll fluorescence in a boreal forest stand  
680 reconstructed from terrestrial laser scanning measurements. *Remote Sens. Environ.* **232**,  
681 111274 (2019).
- 682 118. Albert, L. P. *et al.* Stray light characterization in a high-resolution imaging spectrometer  
683 designed for solar-induced fluorescence. Proc. SPIE 10986, Algorithms, Technologies, and  
684 Applications for Multispectral and Hyperspectral Imagery XXV, 109860G (2019).

- 685 119. Meroni, M. *et al.* Remote sensing of solar-induced chlorophyll fluorescence: Review of  
686 methods and applications. *Remote Sens. Environ.* **113**, 2037-2051 (2009).
- 687 120. Cendrero-Mateo, M. P. *et al.* Sun-induced chlorophyll fluorescence III: Benchmarking  
688 retrieval methods and sensor characteristics for proximal sensing. *Remote Sens.* **11**, 962  
689 (2019).
- 690 121. Vilfan, N. *et al.* Extending Fluspect to simulate xanthophyll driven leaf reflectance  
691 dynamics. *Remote Sens. Environ.* **211**, 345-356 (2018).
- 692 122. Yang, P., Prikaziuk, E., Verhoef, W. & van der Tol, C. SCOPE 2.0: A model to simulate  
693 vegetated land surface fluxes and satellite signals. *Geosci. Model Dev. Discuss.*, 1-26  
694 (2020).
- 695 123. Gastellu-Etchegorry, J. *et al.* DART: recent advances in remote sensing data modeling with  
696 atmosphere, polarization, and chlorophyll fluorescence. *IEEE J. Sel. Top. Appl. Earth Obs.*  
697 *Remote Sens.* **10**, 2640-2649 (2017).

698

699 **Corresponding author:** Albert Porcar-Castell (joan.porcar@helsinki.fi)

700

701 **Acknowledgements:** This perspective idea originated during the Fluorescence Across Space and  
702 Time (FAST) Workshop, which took place in Hyytiälä Forestry Research Station (SMEARII,  
703 Finland) during February 2019. We thank the following participants for active discussions during  
704 the workshop: Juliane Bendig, Kukka-Maaria Erkkilä, Noda Hibiki, Laura V. Junker-Frohn,  
705 Valentyna Kuznetsova, Hannakaisa Lindqvist, Paul Näthe, Jaakko Oivukkamaki, Neus Sabater,  
706 Twinkle Solanki, Tea Thum, Shan Xu and Chao Zhang. We also thank Barry Osmond and Josep  
707 Peñuelas for valuable comments to the manuscript, to Nuria Altimir for improving graphic design  
708 of Figs 1 and 5, and to Bastian Siegmann for the preparation of the HyPlant image in Fig. 3. The

709 Academy of Finland (Project # 288039 and 319211) is acknowledged for the financial support. ZM  
710 was supported by the Australian Research Council (FT160100477), TM was supported by the  
711 National Aeronautics and Space Administration (80NSSC19M0129), and SVW was supported by  
712 the Generalitat Valenciana and the European Social Fund (APOSTD/2018/162). Headwall SIF  
713 images from LPA and JRK were supported by grants from the Institute at Brown for Environment  
714 and Society at Brown University.

715 **Author contributions:** APC conceived the original idea and wrote the manuscript with ZM, TM,  
716 BL, SVW, BFM, FM, YZ, KM with comments and contributions from all co-authors. In addition,  
717 these authors had special contribution to the following parts: Fig.1 (APC, ZM and SVW), Fig.2  
718 (APC, BFM, TM and SVW), Fig. 3 (LPA, UR and JRK), Fig. 4. (APC, ZM, UR, BFM), Fig. 5  
719 (JIGP, JA, ZM, IE), Box 1 (TM, APC), Box 2 (ZM, APC), Supplementary information (ZM, FZ).

720

721

722

723

724

725

726

727

728

729

730 **Figure Legends**

731 **Figure 1. From incoming radiation to observed SIF and photosynthesis: mechanistic**

732 **challenges.** Solar radiation reaching the top of the atmosphere (TOA) is partly absorbed and  
733 scattered by atmospheric gases and particles, decreasing its intensity as it reaches the bottom of the  
734 atmosphere (BOA), generating specific absorption features. Part of the radiation is absorbed by  
735 photosynthetic pigments in vegetation and leaves ( $fAPAR_g$ ) (**Challenge 1**), associated with either  
736 photosystem I (PSI) or photosystem II (PSII), which contribute with differential dynamics and  
737 spectral properties to overall SIF emission (**Challenge 2**). Within each photosystem, energy is  
738 further partitioned into three dynamic processes (**Challenge 3**): i) photochemistry (leading mainly  
739 to linear (LET) or cyclic (CET) electron transport, the latter involving PSI only), ii) thermal energy  
740 dissipation, and iii) ChlaF. Photosynthetic energy (expressed for simplicity in terms of NADPH  
741 equivalents) is further partitioned between alternative energy sinks and gross photosynthesis ( $A_G$ ),  
742 and again between gross primary productivity (GPP) and photorespiration ( $P_R$ ), with dynamics that  
743 are not necessarily seen by SIF (**Challenge 4**). Notably, because it is only possible to measure the  
744 net flux of  $CO_2$  from a leaf or ecosystem, i.e. net photosynthesis or net primary productivity (NPP),  
745 the rate of daytime respiration ( $R_D$ ) must be known or estimated. In turn, because emitted ChlaF  
746 overlaps with the absorption spectra of leaves and plant canopies, some SIF photons - especially  
747 those in the red wavelengths - are re-absorbed within the canopy (**Challenge 5**). Emitted ChlaF is  
748 further scattered and absorbed by aerosols and gases in the atmosphere (**Challenge 6**).

749

750 **Figure 2. The connection between SIF and GPP across space and time.** The relationship

751 between SIF and GPP is affected by multiple factors as we move across spatial and temporal scales.  
752 Some factors exert a similar effect on SIF and GPP, keeping them positively correlated - we call  
753 these couplers. Other factors differentially affect SIF and GPP - we call these decouplers. Factors

754 driving the dynamics of NPQ and APAR will tend to keep SIF and GPP coupled both across space  
755 and time, whereas factors adding variation to the energy partitioning between ChlF and GPP, or  
756 influencing the reabsorption of ChlF, will tend to decouple SIF from GPP (see examples in the  
757 figure). Note how the shape of the ChlF spectrum (“**Spectral dynamics**”) changes across scales in  
758 response to reabsorption within the chloroplast, leaf and canopy, measurable as SIF only within  
759 discrete wavelengths at the canopy and ecosystem levels (Box 1). Equally important to our  
760 understanding of the spatial context of the factors that couple/decouple SIF to GPP is understanding  
761 their temporal range of action (lower panels). For example, the rapid (**second/minute**) decrease in  
762 ChlaF upon saturating illumination of dark acclimated leaves reflects the dynamics of NPQ<sup>76</sup>.  
763 Similar dynamics can be seen under natural conditions at the **diurnal/seasonal** scale in Scots pine  
764 needles, as the quantum yield of fluorescence ( $\Phi F$ ) responds to PQ and NPQ (redrawn from Porcar-  
765 Castell<sup>39</sup>). Here, SIF was estimated for illustrative purposes as  $SIF (r.u.) = PAR \times 0.8 \times 0.5 \times \Phi F$ ,  
766 where 0.8 and 0.5 are estimates for  $fAPAR_g$  and the fraction of radiation absorbed by PSII.  
767 Likewise, **interannual** dynamics at the regional-to-local scales<sup>24</sup> can reflect changes in canopy  
768 structure, physiological stress responses or other functional traits. Ultimately, the challenge of  
769 integrating and disentangling the impact of these couplers/decouplers across space, time, species  
770 and plant stress responses remains (**Challenge 7**).

771

772 **Figure 3.** State-of-the-art SIF imaging methods allow for the observation of SIF across a continuum  
773 of scales: from the leaf-to-individual (top row) to the individual-to-landscape (bottom row). Panel A  
774 shows an RGB image of a senescing maple tree next to an oak tree with green leaves. Panel B  
775 shows the SIF image of the same trees retrieved in the O2A band at 760 nm (SIF760) using a  
776 commercial, off-the-shelf imaging spectrometer<sup>118</sup> mounted on a tripod some meters away and after  
777 applying a filter to exclude non-vegetation pixels (pixels with a normalized difference vegetation  
778 index (NDVI) < 0.65). As expected, the green and photosynthetically active oak emitted SIF at

779 higher magnitude (Panel C) than the senescing maple. Similarly, panels D-E present an airborne  
780 RGB and SIF760 map obtained with data from the HyPlant sensor collected at an altitude of 680 m  
781 above ground<sup>94</sup>. The scene shows several plots within an experimental apple tree plantation at the  
782 agricultural research site Campus Klein-Altendorf (University of Bonn, Germany), where apple tree  
783 varieties of different ages were growing in a typical row structure. Single tree crowns were  
784 segmented by overlaying the SIF images with a 3D surface map and all pixels that were related to a  
785 background signal (defined as ground level + 30 cm) were excluded. The image visualizes the  
786 signal of individual trees, where each pixel corresponds to an area of 1x1 meters and thus the small  
787 clusters represent the signal of an individual tree.

788

789 **Figure 4.** A roadmap towards the standardized interpretation of SIF. The critical steps, data sources  
790 and methods that will be required to overcome the seven challenges are introduced to allow for a  
791 consistent interpretation of spectral observations in terms of leaf, canopy and ecosystem traits.

792

793 **Figure 5.** Potential and emerging SIF applications illustrated in the form of a “SIF-city” metro plan,  
794 where different colors denote five fields of plant science. Identified research applications (metro  
795 stops) are causally connected in individual communication lines, but the final trajectories and  
796 number of stops will depend on how the field of SIF research evolves over the next years. The red-  
797 colored stops denote the application topics elaborated in Section 3.

798

799

800

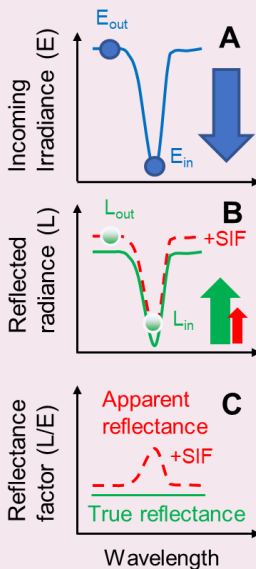
801

802

**Box 1 | Principle of solar-induced fluorescence (SIF) retrieval**

SIF measurements take place outdoors, under ambient sunlight. Accordingly, when pointing a spectroradiometer towards a leaf or plant canopy to make a SIF measurement, we face the challenge that vegetation is highly reflective in the near infrared (NIR) wavelengths, and the signal is dominated by reflected light. The retrieval of SIF from the background reflected radiation is made possible thanks to the spectral properties of incoming light.

The solar spectrum, as measured above a plant canopy, is not continuous; rather, radiation is strongly attenuated within so-called Fraunhofer absorption lines and telluric absorption bands originating from absorption by gases in the Sun's photosphere or the Earth's atmosphere, respectively (see Fig. 1 and an idealized spectral feature in **A**). These features are exploited by the Fraunhofer line depth (FLD) methods<sup>119</sup> where at least four spectral measurements, usually more<sup>120</sup>, are required: the irradiance of the incoming sunlight and the apparent reflected radiance (called apparent, as it includes also SIF), inside and outside of the spectral absorption feature ( $E_{in}/E_{out}$  and  $L_{in}/L_{out}$ , respectively). Since SIF contributes photons similarly both inside and outside the spectral feature (**B**), the relative contribution of SIF to reflected radiation is significantly greater inside the spectral feature, causing an increase in the apparent reflectance (**C**). This increase is proportional to the amount of SIF and can be used to construct a system of equations to retrieve SIF.



Although not mutually exclusive, SIF measurements are often conducted using either the Fraunhofer or Telluric absorption bands, which involve some trade-offs:

- **Fraunhofer lines** (multiple lines across the SIF spectrum). The advantage of these retrievals lies in their lower sensitivity to atmospheric properties, which is practical for remote measurements as well as applications with variable target-to-sensor distances (e.g., multiangular tower measurements). The main disadvantage is that they require spectrometers with extremely high spectral resolutions and generally require longer periods of signal integration.
- **Telluric bands** (mainly oxygen absorption bands B and A, centered around 687-692 nm; and 759-770 nm, respectively). Since these bands are broader, measurements do not require as high spectral resolution and can be also conducted with shorter integration time, which can be especially suitable for some applications (e.g. drone-based observations). Their main disadvantage is that attention must be paid to corrections for atmospheric absorption (Challenge 6).

804

805

806

807

808

809

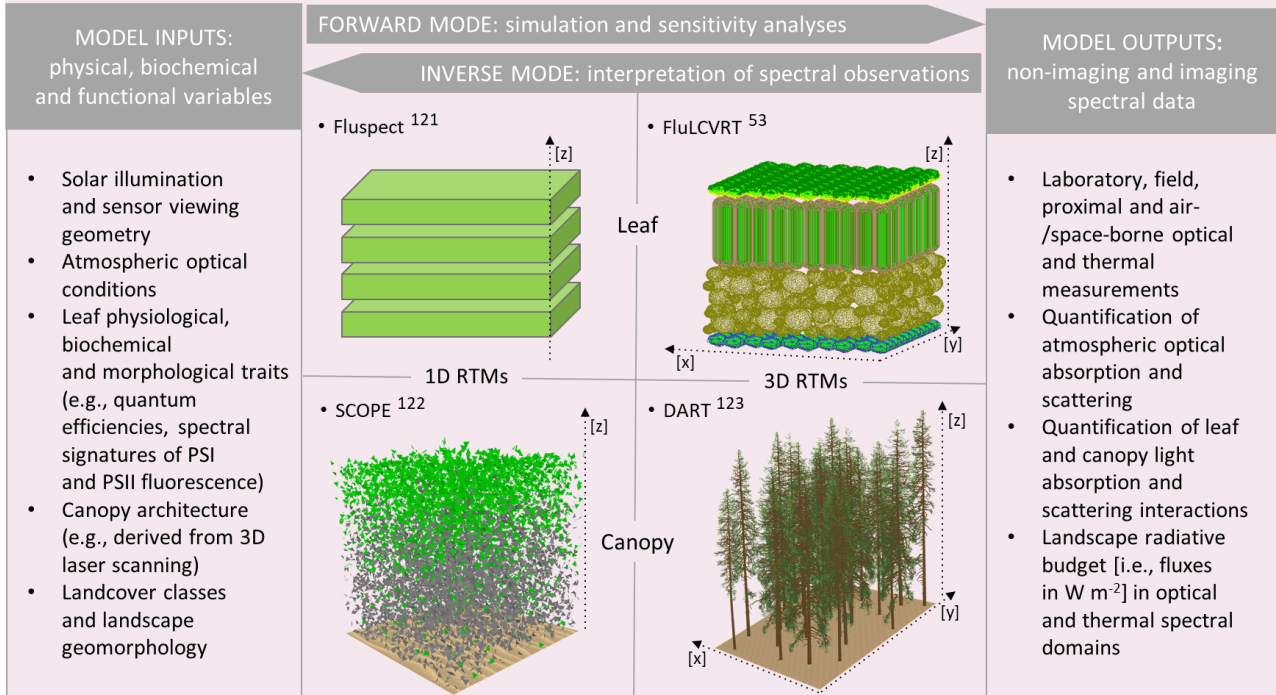
810

811

812

## Box 2 | Radiative transfer models (RTMs)

- **Forward mode.** When the required inputs are provided, RTMs are capable of simulating leaf and canopy SIF together with reflected and emitted optical and thermal radiance. Once successfully validated by independent measurements, RTMs can be used in the forward mode to investigate the sensitivity of outputs, (i.e., surface reflectance and SIF) to different structural, biochemical, and physiological inputs, extending our mechanistic understanding of reflected and emitted photons' propagation across scales.
- **Inverse mode.** RTMs can be also inverted (i.e., run backwards) to estimate from laboratory, field and remote sensing spectral data those leaf and canopy traits that match measured reflectance and SIF data.



- **1D models.** 1D leaf RTMs assume that leaf constituents are horizontally homogeneously distributed in vertically stacked plate structures, and hence require only basic morphological and biochemical inputs (e.g., pigment contents driving PAR absorption and within-leaf reabsorption, the intrinsic PSII and PSI fluorescence spectra, and the dynamics in the quantum yield of fluorescence as the mechanistic link to photosynthesis). This simplicity, however, ignores potentially important factors, such as within-leaf heterogeneity or chloroplast movements. As with the 1D leaf construct, 1D canopy RTMs assume that vegetation can be represented by horizontally homogeneous layers filled with leaves of a predefined size, density and geometry (angular distribution), which allows for minimal model inputs and a relatively straightforward application. The 1D architecture has its uses for spatially homogeneous canopies (e.g., crops).
- **3D models.** Structurally complex leaves and spatially heterogeneous plant communities (e.g., forests and savannas) require 3D representations. 3D leaf RTMs can model optical interactions within a genuine 3D digital representation of leaf interior reconstructed, for example, with imaging tomography or confocal microscopy. As demonstrated in the Supplementary Videos 1 and 2, 3D RTM solutions also exist for spatially diversified plant canopies, allowing for accurate physical simulations of  $APAR_g$  and SIF fluxes in complex canopies.

813

814

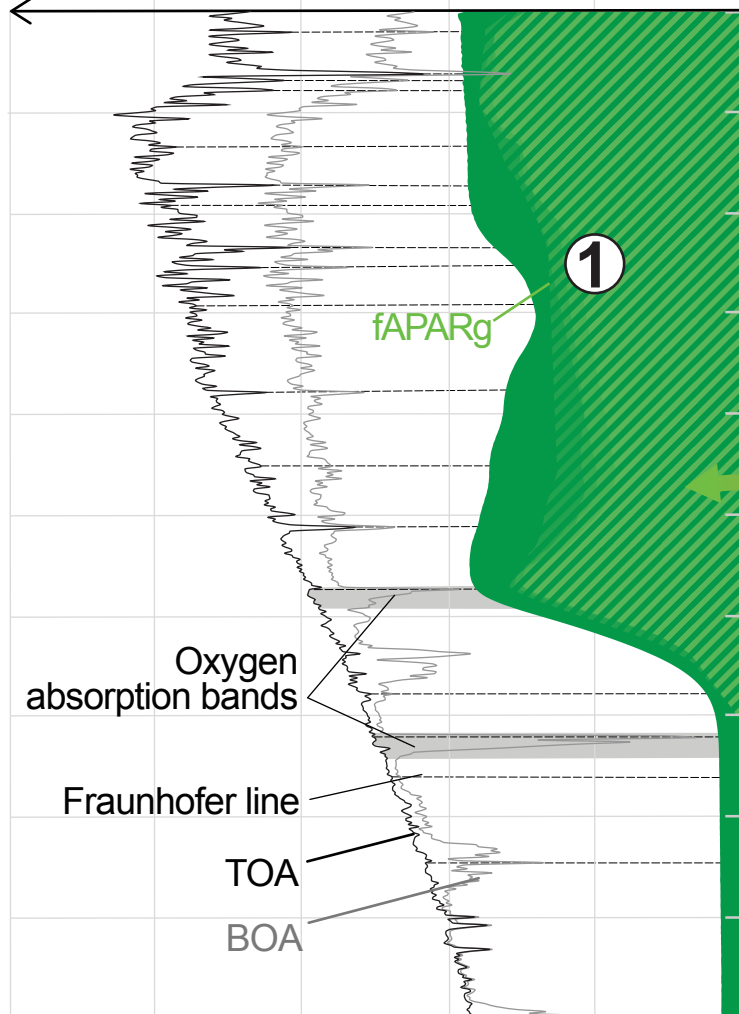
815



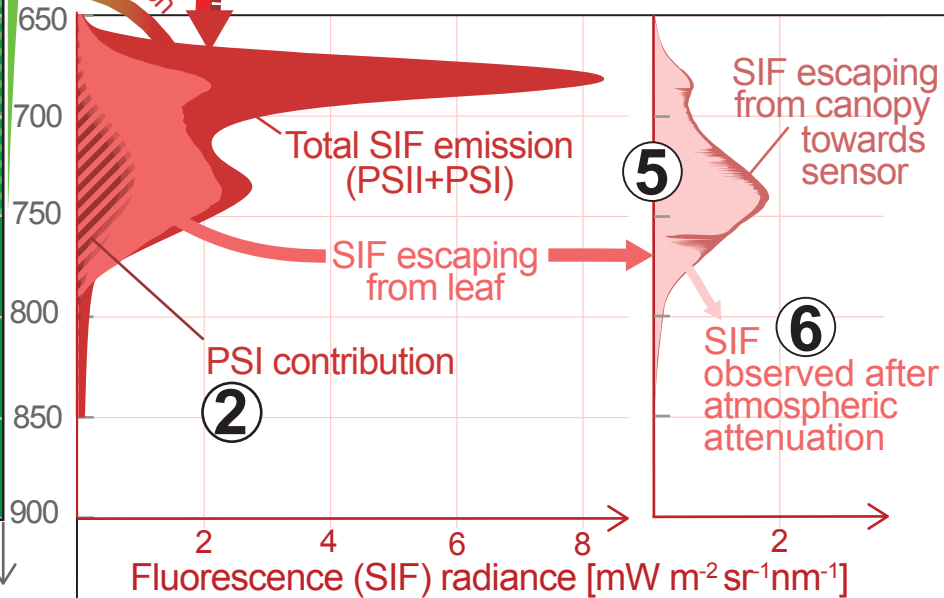
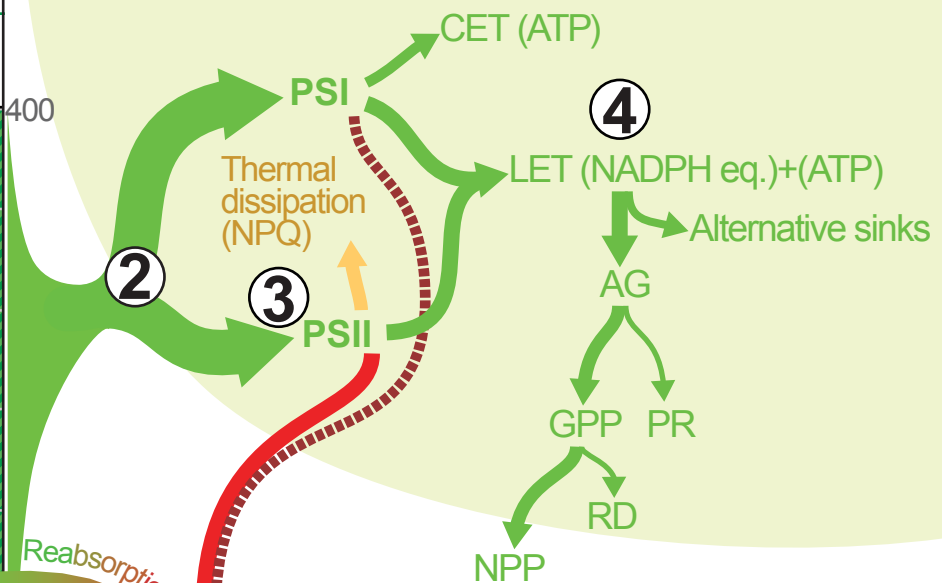
# EXCITATION

Solar spectral irradiance  
[W m<sup>-2</sup> nm<sup>-1</sup>]

← 2 1.5 1



# PHOTOSYNTHETIC ENERGY PARTITIONING



# EMISSION

